Article

Picosecond Kinetic Study of the Photoinduced Homolysis of Benzhydryl Acetates: The Nature of the Conversion of Radical Pairs into Ion Pairs

Libby R. Heeb, and Kevin S. Peters

J. Am. Chem. Soc., **2008**, 130 (5), 1711-1717 • DOI: 10.1021/ja077105n

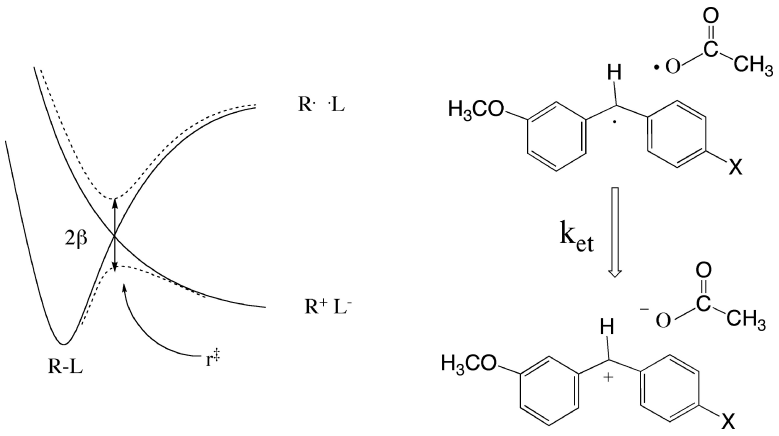

More About This Article

Additional resources and features associated with this article are available within the HTML version:

- Supporting Information
- Access to high resolution figures
- Links to articles and content related to this article
- Copyright permission to reproduce figures and/or text from this article

View the Full Text HTML

J|A|C|S
ARTICLES
Published on Web 01/11/2008

Picosecond Kinetic Study of the Photoinduced Homolysis of Benzhydryl Acetates: The Nature of the Conversion of Radical Pairs into Ion Pairs

Libby R. Heeb and Kevin S. Peters*

Department of Chemistry and Biochemistry, University of Colorado, Boulder, Colorado 80309

Received September 13, 2007; E-mail: Kevin.Peters@Colorado.Edu

Abstract: The conversion of benzhydryl acetate geminate radical pairs to contact ion pairs following photoinduced homolysis in solution is studied using picosecond pump−probe spectroscopy. The dynamics for the decay of the geminate radical pairs into contact ion pairs is modeled within a Marcus-like theory for nonadiabatic electron transfer. A second decay channel for the geminate radical pairs is diffusional separation to free radicals. The kinetics of this latter process reveals an energy of interaction between the two radicals in the geminate pair.

Introduction

Bond heterolysis and bond homolysis are two of the most fundamental reaction processes found in organic chemistry. The mechanistic elucidation of these reaction processes began in the 1930s with the pioneering experimental studies of Hughes and Ingold and continues to be an active area of research.[1−7] Theoretical consideration of these reaction processes began in 1935 with the seminal work of Ogg and Polanyi which has since been significantly expanded upon by Pross, Shaik, Warshel, and Hynes.[8−11] At its most basic level, the reaction energy surface is developed within the context of two diabatic states, a homopolar covalent state and an ionic state, Scheme 1.

In the gas phase and in nonpolar solvents, the dissociation on the ground state surface leads to the formation of a radical pair, R • • L, while dissociation on the excited-state surface leads to the formation of an ion pair, R^+ L^-. In a polar solution, differential solvation of the two diabatic states leads to the stabilization of the ionic surface relative to the homopolar covalent surface so that, at distances associated with dissociated product, the ion pair is more stable than the radical pair. At the point of crossing of the two diabatic states (solid curves) in polar solution, a resonant interaction between the two states leads to the generation to two adiabatic surfaces (dashed curves); the magnitude of the resonance interaction is characterized by the term β, and the resultant energy splitting between the two adiabatic surfaces is 2β. Within the Ogg−Polanyi model, the transition state for bond heterolysis in polar solution occurs at a distance associated with the crossing of the two diabatic states, $r^{\ddagger}$.[8]

For the past 10 years our research group has addressed numerous questions that arise from the contemplation of the potential energy curves depicted in Scheme 1.[2,3,12−18] The molecular system most often employed in our studies has been derivatives of benzhydryl chlorides, bromides, and acetates. Using femtosecond laser methodologies, the partitioning of the first excited singlet state into radical pairs and ion pairs has been probed for benzhydryl chloride, reaction processes that occur on the 300 to 800 femtosecond time scale.[15] The mechanism of this partitioning was discussed within the context of conical intersections; further studies are still required to gain a fuller understanding of the partitioning processes. On the picosecond time scale, the collapse of the contact ion pair to form a covalent bond and the competing diffusional separation to form the solvent-separated ion pair were extensively studied.[18] The dynamics for the passage through the transition state associated with covalent bond formation from the contact ion pair was found to deviate substantially from the predictions of transition state theory; interpretation of the kinetics within the context of Hynes theory for polarization caging revealed that passage through the transition state is strongly coupled to and often controlled by solvent motion.[19]

(1) Bateman, L. C.; Hughes, E. D.; Ingold, C. K. *J. Chem. Soc.* **1940**, 1017−1026.
(2) Peters, K. S. *Chem. Rev.* **2007**, *107*, 859−873.
(3) Peters, K. S. *Acc. Chem. Res.* **2007**, *40*, 1−7.
(4) Richard, J. P.; Amyes, T. L.; Toteva, M. M.; Tsuji, Y. In *Advances in Physical Organic Chemistry*; Richards, J. P., Ed.; Elsevier: Amsterdam, 2004; Vol. 39.
(5) Mayr, H.; Patz, M. *Angew. Chem., Int. Ed.* **1994**, *33*, 938−957.
(6) Minegishi, S.; Loos, R.; Kobayashi, S.; Mayr, H. *J. Am. Chem. Soc.* **2005**, *127*, 2641−2649.
(7) Tsuji, Y.; Toteva, M. M.; Garth, H. A.; Richard, J. P. *J. Am. Chem. Soc.* **2003**, *125*, 15455−15465.
(8) Ogg, R. A.; Polanyi, M. *Trans. Faraday Soc.* **1935**, *31*, 604−620.
(9) Pross, A.; Shaik, S. S. *Acc. Chem. Res.* **1983**, *16*, 363−370.
(10) Warshel, A. *Acc. Chem. Res.* **1981**, *14*, 284−290.
(11) Kim, H. J.; Hynes, J. T. *J. Am. Chem. Soc.* **1992**, *114*, 10508−10528.
(12) Peters, K. S.; Li, B. *J. Phys. Chem.* **1994**, *98*, 401−403.
(13) Lipson, M.; Deniz, A. A.; Peters, K. S. *J. Phys. Chem.* **1996**, *100*, 3580−3586.
(14) Lipson, M.; Deniz, A. A.; Peters, K. S. *J. Am. Chem. Soc.* **1996**, *118*, 2992−2997.
(15) Lipson, M.; Deniz, A. A.; Peters, K. S. *Chem. Phys. Letts.* **1998**, *288*, 781−784.
(16) Dreyer, J.; Lipson, M.; Peters, K. S. *J. Phys. Chem.* **1996**, *100*, 15162−15164.
(17) Dreyer, J.; Peters, K. S. *J. Phys. Chem.* **1996**, *100*, 15156−15161.
(18) Peters, K. S.; Gasparrini, S.; Heeb, L. R. *J. Am. Chem. Soc.* **2005**, *127*, 13039−13047.
(19) Zwan, G. v. d.; Hynes, J. T. *J. Chem. Phys.* **1982**, *76*, 2993−3001.

Scheme 1.

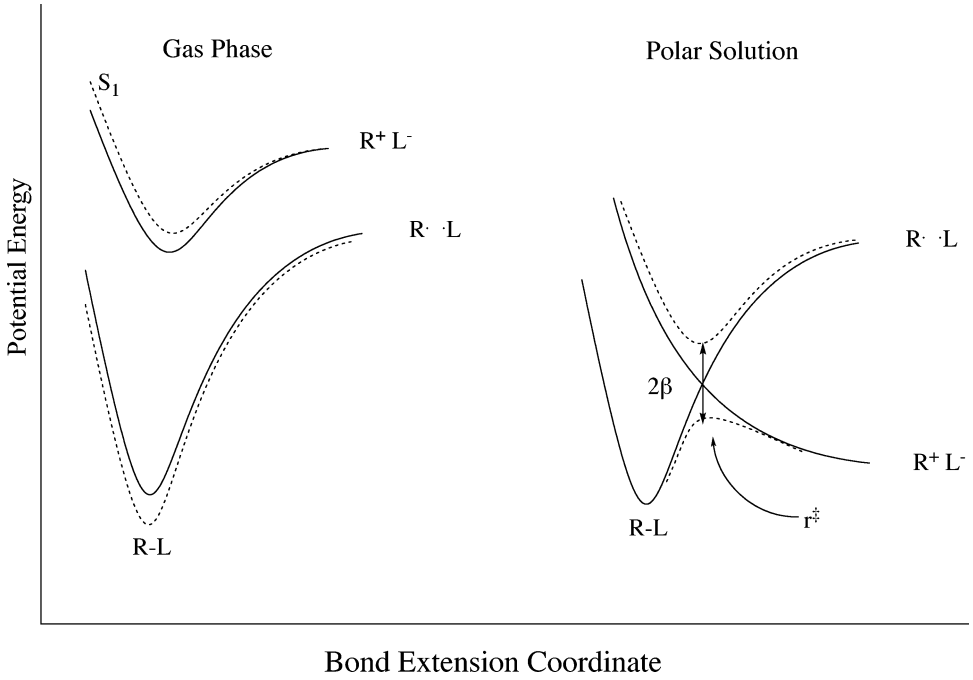

Several questions remain to be addressed. The valence bond diagram of Scheme 1 would suggest that, in polar solution, the geminate radical pair located directly above the transition state for ground state bond heterolysis should experience a stabilizing electronic interaction; the magnitude of this stabilization has yet to be addressed. Also the energy splitting associated with the two adiabatic surfaces at the transition state for bond heterolysis has yet to be determined. Finally the mechanism by which the geminate radical pair, which resides on an excited-state surface, decays into a contact ion pair remains to be fully elucidated. The aim of the present study is to address these three questions.

The question as to the mechanism by which a radical pair decays into an ion pair was initially raised and extensively investigated by Pincock and co-workers.[20,21] Based upon the analysis of yields of photosolvolysis products of arylmethyl esters, they found that the mechanism for the decay of the radical pair into an ion pair follows the predictions of a modified Marcus model for nonadiabatic electron transfer. The kinetics of electron transfer were abstracted from the product yields by assuming values for the rate constant for radical pair diffusional separation and decarboxylation of the ester radical.

Experimental Section

Chemicals. The solvents acetonitrile (99.8%), propionitrile (99%), and butyronitrile (99+%) were purchased from Aldrich and used as received; for solvent hazards see Supporting Information. Five molecules were employed in the study: (3-methoxyphenyl)(4-methoxyphenyl)methyl acetate (4-CH_3O), (3-methoxyphenyl)(*p*-tolyl)methyl acetate (4-CH_3), (3-methoxyphenyl)(phenyl)methyl acetate (4-H), (4-(trifluoromethyl)phenyl)(3-methoxyphenyl)methyl acetate (4-CF_3), and (4-cyanophenyl)(3-methoxyphenyl)methyl acetate (4-CN).

The syntheses of these molecules as well as their NMR and high-resolution mass spectral characterizations are detailed in the Supporting Information.

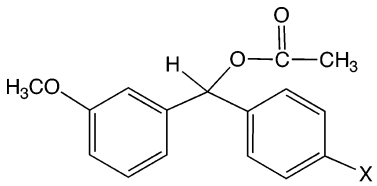

X
4- CH_3O
4- CH_3
4-H
4-CF_3
4-CN

Kinetics Apparatus. The time-dependent absorbance of the probe wavelength was measured using a picosecond laser system, described in previous papers.[22] This system employs a Continuum Leopard D-10 laser with an 8 ps pulse length. Samples were contained in a 1 cm path length quartz cuvette at room temperature with a magnetic stir bar. The optical density of the samples of benzhydryl acetates measured at 266 nm varied between 1.5 OD to 2.0 OD. The samples were irradiated with 266 nm and probed at 355 nm.

The time-dependent absorbance obtained from the kinetic experiments results from the convolution of an instrument response function, $I(t)$, with the molecular kinetics, $F(t)$, and is given by[22]

$$A(t) = \int_{-\infty}^{t} I(\tau)\, F(t-\tau)\, \mathrm{d}\tau \qquad (1)$$

The instrument response function is the result of a convolution of the pump and probe beams and is assumed to have the analytical form of a Gaussian,

$$I(t) = (2\pi\sigma)^{-0.5} \exp(-(t - t_0)/2\sigma^2 \qquad (2)$$

The kinetic parameters are solved for simultaneously employing the downhill simplex method to minimize the sum of the square of the residuals.

(20) DeCosta, D. P.; Pincock, J. A. *J. Am. Chem. Soc.* **1989**, *111*, 8948−8950.
(21) Hilborn, J. W.; MacKnight, E.; Pincock, J. A.; Wedge, P. J. *J. Am. Chem. Soc.* **1994**, *116*, 3337−3346.
(22) Peters, K. S.; Lee, J. *J. Phys. Chem.* **1993**, *97*, 3761−3764.

Scheme 2.

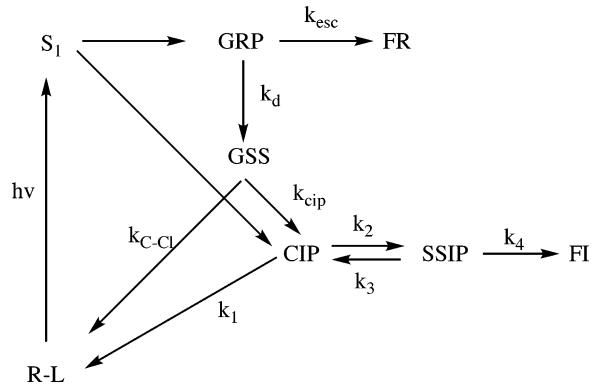

Calculations. The calculated electronic energies for 4-CH_3O and 4-CN as well as their associated radicals and cations are based upon B3LYP density functional theory at the 6-31G* level using Spartan 04. The electronic energies and coordinates are given in the Supporting Information. The calculated vibrational frequencies employed AM1 using Spartan 04; the derived values for the vibrational frequencies were scaled by a factor of 0.9.[23]

Results

Prior kinetic studies have established the following reaction scheme for the photoinduced bond homolysis and bond heterolysis of benzhydryl acetates, Scheme 2.[18]

The first excited singlet state, S_1, decays by partitioning between the geminate radical pair, GRP, and the contact ion pair, CIP, on the 100 fs time scale. The GRP decays by two reaction pathways: diffusional separation, k_{esc}, to form free radicals (FR), and a transition onto the ground state surface (GSS), k_d. Once on the ground state surface, the system evolves into the CIP or reforms the initial reactant, R−L. In turn, the CIP collapses, k_1, to reform the initial reactant R−L through the formation of a covalent bond or undergoes diffusional separation to the solvent separated ion pair (SSIP), k_2. The SSIP decays by diffusional separation to free ions (FI), k_4, or collapses to reform the CIP, k_3.

The time evolution of the benzhydrylium radicals and the benzhydrylium cations is monitored through the absorption spectrum of each species. Steenken and co-workers, employing nanosecond absorption spectroscopy, have determined that the variously substituted benzhydrylium radicals absorption maxima range from 330 to 350 nm.[24] The absorption spectra of the variously substituted benzhydrylium cations are well separated from that of the radicals and have absorption maxima ranging from 440 to 500 nm. In the present series of experiments, we examine the dynamics of the substituted benzhydrylium radicals using 355 nm probe, given the convenience of the third harmonic of YAG. For several of the derivatives we checked the kinetics of the radicals at 340 nm and have found them to be identical to those measured at 355 nm.

Acetonitrile, propionitrile, and butyronitrile solutions of 4-CH_3O, 4-CH_3, 4-H, 4-CF_3, and 4-CN were irradiated at 266 nm, and the dynamics of the transient species were monitored at 355 nm. An example of time evolution of the radical produced upon photolysis of 4-CH_3O in acetonitrile is shown in Figure 1. The radical decays exponentially on the 1 ns time scale to a constant absorbance that persists beyond the 4 ns time scale, the end of the time duration of the experiment. Similar behavior is observed for each species of radical.

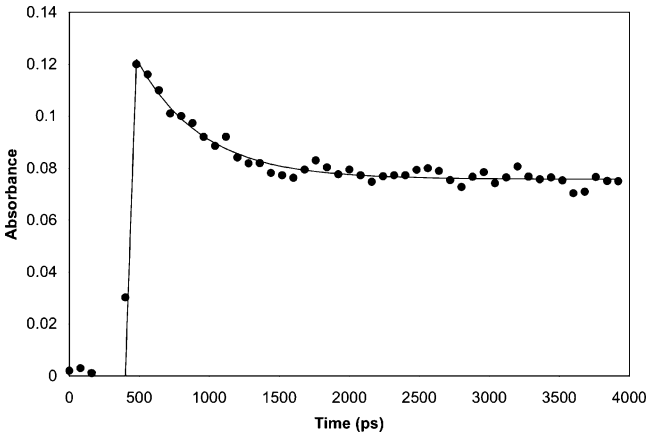

Figure 1. Absorbance data showing decay of (3-methoxyphenyl)(4-methoxyphenyl)methyl acetate (4-CH_3O) radical pair absorbance at 355 nm in acetonitrile. Solid lines represent Scheme 3 fit, with $k_d = 8.97 \times 10^8\ s^{-1}$ and $k_{esc} = 1.25 \times 10^9\ s^{-1}$.

Scheme 3.

The radical decays are fit to the model depicted in Scheme 3 with the assumption that the extinction coefficients for GRP and FR are the same at 355 nm.

The model predicts a single-exponential decay for the GRP with a rate constant equal to the sum of k_d and k_{esc}. The yield of FR on the 4 ns time scale is given by

$$[FR]_{4ns} = \frac{k_{esc}}{k_{esc} + k_d}[\mathrm{GRP}]_0 \qquad (3)$$

An example of the fit to the model described by Scheme 3 to the experimental data is shown in Figure 1. The resulting kinetic parameters for the decay of the five radical species in each of the three solvents are given in Table 1. In acetonitrile, the rate constants for decay onto the GSS, k_d, vary by a factor of 44, from $8.9 \times 10^8\ s^{-1}$ to $3.9 \times 10^{10}\ s^{-1}$, while the rate constants for diffusional separation, k_{esc}, vary by a factor of 14.3, from $1.3 \times 10^9\ s^{-1}$ to $1.86 \times 10^{10}\ s^{-1}$. At first glance, the variation in k_{esc} by a factor of 14.3 is rather surprising.

Discussion

Kim−Hynes Model. Understanding the trends evident in k_{esc} and k_d with changing benzhydryl substituents requires insight into the topography of the potential energy surfaces for the ion pairs and radical pairs as well as knowledge of where the radical to ion pair conversion is occurring on these surfaces. The energy surfaces developed in a theoretical study of the S_N1 reaction mechanism for *tert*-butyl chloride by Kim and Hynes are employed to gain insight into the source of the trends observed in the experiments.[11,25−28] Starting with the two gas-phase diabatic surfaces of Ogg and Polyani (Scheme 1), the Kim−Hynes model incorporates the interaction of the valence bond states with the solvent polarization under equilibrium and

(23) Hehre, W. J.; Yu, J.; Klunzinger, P. E.; Lou, L. *A Brief Guide to Molecular Mechanics and Quantum Chemical Calculations*; Wavefunction, Inc.: Irvine, CA, 1998.
(24) Bartl, J.; Steenken, S.; Mayr, H.; McClelland, R. A. *J. Am. Chem. Soc.* **1990**, *112*, 6918−6928.

Table 1. Kinetic Parameters from Scheme 3 for the Geminate Radical Pair Dynamics Associated with 4-MeO, 4-Me, 4-H, 4-CF_3, and 4-CN as a Function of Solvent at 23 °C

solvent	acetonitrile		propionitrile		butyronitrile	
4′-substituent	k_d (s^{-1})[a]	k_{esc} (s^{-1})	k_d (s^{-1})	k_{esc} (s^{-1})	k_d (s^{-1})	k_{esc} (s^{-1})
CH_3O	8.97×10^8	1.25×10^9	6.80×10^8	8.50×10^8	6.56×10^8	1.12×10^9
CH_3	3.22×10^9	1.55×10^9	2.58×10^9	1.44×10^9	3.10×10^9	1.96×10^9
H	5.04×10^9	1.54×10^9	3.77×10^9	1.75×10^9	3.73×10^9	2.16×10^9
CF_3	3.96×10^{10}	1.86×10^{10}	1.79×10^{10}	1.69×10^{10}	1.28×10^{10}	1.18×10^{10}
CN	2.80×10^{10}	8.09×10^9	2.63×10^{10}	1.31×10^{10}	2.21×10^{10}	1.34×10^{10}

[a] Uncertainties in fits are ± 10% (1σ).

Scheme 4.

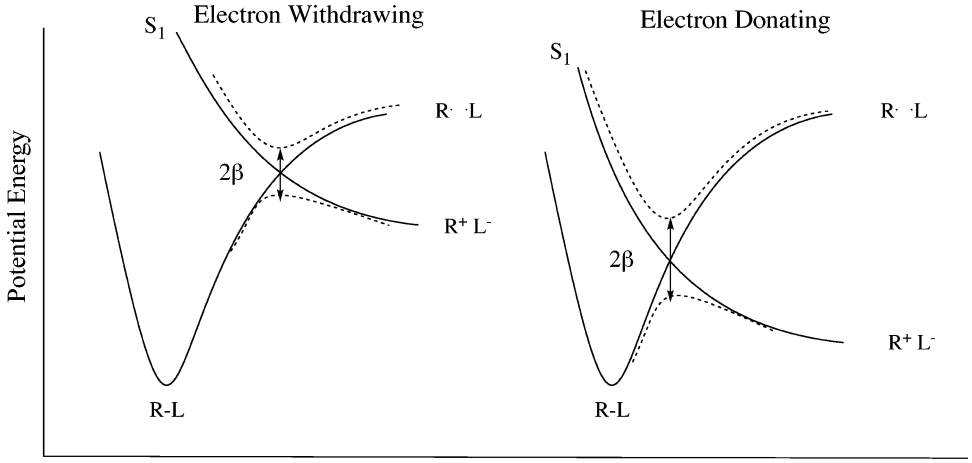

nonequilibrium conditions; the two surfaces are then coupled through a nonlinear Schrodinger formalism to produce two adiabatic surfaces. The adiabatic surfaces are a function of two fundamental reaction coordinates: the bond stretch coordinate, *r*, and the collective solvent coordinate, s. The dielectric continuum model used to describe the solvent is a function of the solvent electronic polarization, P_{el}, and the solvent orientational polarization, P_{or}.

Of the numerous important findings obtained by Kim and Hynes, findings that significantly change the description of the transition state for the S_N1 reaction mechanism in terms of charge distribution and solvent polarization, the one finding of importance to the present study, is depicted in Scheme 4.[11]

As the diabatic excited-state surface that correlates with the ion pair R^+L^- is progressively stabilized relative to the diabatic ground state covalent curve, the crossing of the two diabatic curves occurs at shorter bond extensions in R−L. As the diabatic surfaces (solid curve) crossing point moves to shorter distances, the electronic coupling between the two surfaces, β, increases in magnitude so that the splitting, 2β, between the two resulting adiabatic surfaces (dashed curves) increases. Furthermore the depth of adiabatic well on the excited-state surface increases with the stabilization of the ionic surface; it is in this well that the geminate radical pair resides and whose position in the bond extension coordinate is directly above the region of the transition state for bond heterolysis.

In the Kim−Hynes study, stabilization of the ionic surface relative to the covalent surface was effected by an increase in solvent polarity.[11] However, changing the substituents on the benzhydryl moiety from electron withdrawing (i.e., CF_3, CN) to electron donating (i.e., MeO, Me) will also increase the stabilization of the benzhydrylium cation diabatic surface relative to the benzhydrylium radical diabatic surface. Thus, based on the Kim−Hynes model, as the substituents are changed from electron withdrawing to electron donating, the energy splitting between the transition state on the ground state surface for bond heterolysis and the geminate radical pair residing directly above the transition state should increase. This change in substituents will also increase the potential energy well depth for the geminate radical pair relative to the dissociated free radicals. The existence of a potential energy well for the geminate radical pair implies that there is a stabilizing energy of interaction within the geminate radical pair relative to the free radicals; the magnitude of the interaction has yet to be quantified.

Stabilization Energy of the Geminate Radical Pair. The proposal that the geminate radical pair is stabilized by an electronic interaction, whose origin is traced to the resonance hybrid interaction between the covalent−ionic diabatic surfaces, is not new. In 1970, Walling and co-workers reported a study of the distribution of products resulting from the thermal decomposition of diacyl peroxides in solvents of varying polarity.[29] Following the passage through the transition state for peroxide decomposition, Walling proposed that "they pass to an intimate or tight ion pair−radical pair intermediate in which electronic interaction between the fragments is still extensive and ionic and paired diradical formulations merely represent contributing structures of a resonance hybrid."[29] This

(25) Kim, H. J.; Hynes, J. T. *J. Am. Chem. Soc.* **1992**, *114*, 10528−10537.
(26) Mathis, J. R.; Hynes, J. T. *J. Phys. Chem.* **1994**, *98*, 5445−5459.
(27) Mathis, J. R.; Hynes, J. T. *J. Phys. Chem.* **1994**, *98*, 5460−5470.
(28) Mathis, J. R.; Kim, H. J.; Hynes, J. T. *J. Am. Chem. Soc.* **1993**, *115*, 8248−8262.
(29) Walling, C.; Waits, H. P.; Milovanovic, J.; Pappiaonnou, C. G. *J. Am. Chem. Soc.* **1970**, *92*, 4927−4932.

description captures the essence of the Kim−Hynes theoretical formulation for the electronic structure of the geminate radical pair.

The energy difference between the geminate radical pair and its solvent separated form, defined here as the free radicals, has yet to be established directly. However, consideration of the rate constants for the diffusional separation of the GRP to the FR, k_{esc}, provides insight into the energy of interaction. If a model for the diffusional separation rate of the GRP, in which there is no electronic interaction within the GRP, can be developed, then comparison of this hypothetical rate constant with the series of observed k_{esc} will provide an estimate of the energy of interaction. Gardiner developed a theoretical model for the diffusional separation of a noninteracting geminate radical pair; the rate constant is given by

$$k_{esc} = \frac{3(D_A + D_B)}{(r_A + r_B)^2} \quad (4)$$

where D_A and D_B are the diffusion coefficients for the two radical fragments, and r_A and r_B are the radii of the two fragments.[30] This hypothetical rate constant represents an upper bound for the rate constant associated with the diffusional separation of a geminate radical pair.

The diffusion coefficient of the benzhydryl radical in *n*-hexane has been determined. Arita and co-workers measured the kinetics for the self-coupling of the benzhydrylium radical; analysis of the kinetics within the Smoluchowski theory for diffusion-controlled reactions yields a diffusion coefficient of 1.7×10^{-9} $m^2\ s^{-1}$.[31] Since the diffusion coefficient is inversely proportional to the viscosity, the diffusion coefficient in acetonitrile is estimated to be 1.5×10^{-9} $m^2\ s^{-1}$ given the viscosities of acetonitrile (0.36 cps) and *n*-hexane (0.30 cps).[32] While the diffusion coefficient for the acetate radical has not been measured, the diffusion coefficient of acetic acid should be similar.[33,34] In ethyl acetate (0.441 cps), the value is 2.18×10^{-9} $m^2\ s^{-1}$ leading to an extrapolated diffusion coefficient of 2.7×10^{-9} $m^2\ s^{-1}$ in acetonitrile. An estimate of the radii for the two radical species is made by calculating the molecular volume of the fragments, obtained using Spartan at the AM1 level, and then calculating the radius of a sphere for the same volume. The calculation leads to radii of 3.5 Å for the benzhydrylium radical and 2.28 Å for the acetate radical. Based on eq 4, the hypothetical rate constant for the diffusional separation of the noninteracting geminate radical pair is 3.9×10^{10} s^{-1}.

If it is assumed that the difference between the hypothetical rate constant for diffusional separation of noninteracting geminate radical pairs and the experimentally observed rate constants for diffusional separation is traced to the electronic interaction within the geminate radical pair, then the energy of interaction can be estimated. Assuming that there is no electronic interaction between the radicals within the transition state for GRP diffusional separation and assuming a common A factor for the separation, the ratio of the experimental rate constant, k_{esc}(expt), to the modeled noninteracting rate constant, k_{esc}(calcd), yields the energy of interaction, ΔE_{int}, defined as a positive quantity.

$$\frac{k_{esc}(\text{expt})}{k_{esc}(\text{calcd})} = \exp(-\Delta E_{int}/RT) \quad (5)$$

The values of ΔE_{int} are given in Table 2 for the solvents acetonitrile, propionitrile (0.42 cps), and butyronitrile (0.58 cps) where the viscosity dependence of k_{esc}(calcd) has been taken into account.[35] As predicted by the diagram in Scheme 4, when electron withdrawing substituents are replaced by electron donating substituents, leading to a decrease in the distance of the crossing points between the diabatic surfaces, there is an increase in energy of the well depth associated with the GRP. Relative to a noninteracting GRP, the energy of interaction within the GRP is not large, only ranging from 0.4 kcal/mol (CF3) to 2.0 kcal/mol (MeO) in acetonitrile. The effect of this small variation in the energy of interaction leads to a change in k_{esc} by a factor of 15.

Table 2. Electronic Energy of Interaction, ΔE_{int}, within the Geminate Radical Pair for 4-CH_3O, 4-CH_3, 4-H, 4-CF_3, and 4-CN as a Function of Solvent

solvent	acetonitrile	propionitrile	butyronitrile
4′-substituent	ΔE_{int} (kcal/mol)	ΔE_{int} (kcal/mol)	ΔE_{int} (kcal/mol)
CH_3O	2.0	2.1	1.8
CH_3	1.9	1.8	1.5
H	1.9	1.7	1.4
CF_3	0.4	0.4	0.4
CN	0.9	0.5	0.3

Electronic Coupling for the Diabatic Surfaces. The Kim−Hynes study of the S_N1 reaction mechanism cast in terms of valence bond reaction diagrams reveals that as the ionic surface is stabilized relative to the covalent surface, the position of the transition state for bond heterolysis decreases and, importantly, the electronic coupling between the two diabatic surfaces increases leading to a larger splitting between the two adiabatic surfaces, Scheme 4. For the series *tert*-butyl iodide, *tert*-butyl bromide, and *tert*-butyl chloride in acetonitrile, as the position of the transition state for bond heterolysis decreases (2.83, 2.65, and 2.49 Å), the splitting between the two adiabatic surfaces, 2β, increases (8.1, 27.8, and 35.4 kcal/mol).[28]

Combining the information obtained in the present study with our prior studies, we calculate the energy separation between the GRP and transition state for bond heterolysis, the difference reflecting the value of 2β. In ref 18, we present the methodology for determining the energy of the contact ion pair (CIP) and the free radical pair (FR) for 4-CH_3O, 4-CH_3, and 4-H. The same procedure is used herein for 4-CF_3 and 4-CN. In the same study, from the temperature dependence of the rate constant for the collapse of the contact ion pair to form the covalent bond, the energy of the transition state for bond heterolysis of 4-CH_3O, 4-CH_3, and 4-H is determined. Finally, the energy of the GRP is obtained from the calculated energy of the FR and the stabilization energy given in Table 2. The energies for the various species in acetonitrile along with the energy for the

(30) Gardiner, W. C. *Rates and Mechanisms of Chemical Reactions*; W.A. Benjamin, Inc: New York, 1969.
(31) Arita, T.; Kajimoto, O.; Terazima, M. *J. Chem. Phys.* **2004**, *120*, 7071−7074.
(32) *CRC Handbook of Chemistry and Physics*; Lide, D. R., Ed; CRC Press: Boca Raton, FL, 2001.
(33) Terazima, M.; Tenma, S.; Watanabe, H.; Tominaga, T. *J. Chem. Soc., Faraday Trans.* **1996**, *92*, 3057−3062.
(34) Lewis, J. B. *J. Appl. Chem.* **1955**, *5*, 228−237.
(35) Li, B.; Peters, K. S. *J. Phys. Chem.* **1993**, *97*, 7648−7651.

Table 3. Energy of the Contact Ion Pair (CIP), the Transition State (TS), Free Radicals (FR), Geminate Radical Pair (GRP), and Splitting of the Adiabatic Surfaces (2β) for 4-CH_3O, 4-CH_3, 4-H, 4-CF_3, and 4-CN in Acetonitrile

4′-substituent	CIP (kcal/mol)	TS for CIP (kcal/mol)	FR (kcal/mol)	GRP (kcal/mol)	2β (kcal/mol)
CH_3O	21.3	26.7	58.9	56.9	30.2
CH_3	27.0	30.2	59.0	57.1	26.9
H	30.8	32.7	59.1	57.2	24.5
CF_3	40.4	41.4[a]	61.5	61.1	19.7
CN	42.9	43.9[a]	60.6	59.7	15.8

[a] Estimated based on data for MeO, Me, and H.

splitting between the two adiabatic surfaces are given in Table 3. As electron-withdrawing substituents are replaced with electron-donating substituents serving to stabilize the ionic surface relative to the covalent surfaces, the splitting 2β increases from 15.8 kcal/mol (4-CN) to 30.2 kcal/mol (4-CH_3O), a trend supported by Kim−Hynes valence bond calculations.

Conversion of GRP to CIP. Pincock and co-workers first addressed the mechanism for the geminate radical pair transformation into a contact ion pair.[20,21] Examining the product distributions resulting from the photolysis of 1-naphthylmethyl esters and benzyl acetates, they proposed that conversion of the radical pair to an ion pair be viewed as a nonadiabatic electron-transfer process. The kinetics of the transformation were correlated with the driving force for electron transfer; the rate constants for electron transfer were derived from product yields, an assumed value for the rate constant for decarboxylation of the ester radical, and an assumed rate constant for diffusional separation of the radical pair. Both a normal region and an inverted region were observed for the electron transfer which were analyzed within the context of nonadiabatic electron transfer theory. The decay of the geminate radical pair by electron transfer was viewed as directly giving rise to the contact ion pair.

In our earlier study of the picosecond dynamics of bond homolysis of benzhydryl chloride and benzhydryl bromide giving rise to the geminate radical pair, we proposed that the transition from the geminate radical pair onto the ground state surface occurs in the region of the transition state for bond heterolysis; the contact ion pair is not directly formed from the geminate radical pair, Scheme 2.[14,17] The proposal was based upon the valence bond diagram developed by Kim and Hynes as well as the quantum yields for the production of the various reactive species. Returning to Scheme 4, the transition of the geminate radical pair onto the ground state surface that requires the least amount of internal molecular rearrangement would place the system in the region of the transition state for ground state bond heterolysis. Furthermore if the GRP were to evolve directly into the CIP through electron transfer, the GRP would first have to undergo an increase in separation along the R−L elongation coordinate. This motion is a thermally activated event, and in addition, this elongation would serve to reduce the electronic coupling between the two radical species, leading to a retardation in the rate of electron transfer. Experimental substantiation of this proposal can be found in the analysis of the quantum yields for the production of radical pairs and ion pairs.[17] Combining the quantum yields studies of Steenken and co-workers with our picosecond measurements, the final product distribution is only consistent with the proposal that the transition of the GRP onto the ground state surface, GSS, occurs in the region of the transition state for bond heterolysis, Scheme 2.[24] Once on the ground surface, the system then partitions between reformation of the covalent bond and contact ion pair formation.

A transition between electronic states that places a system in the transition state of a reactive coordinate is not a novel proposal. Lineberger, Borden and co-workers measured the photoelectron spectrum for the transition of cyclooctatetraene radical anion to the $^1A_{1g}$ state of cyclooctatetraene (COT) with D_{4h} symmetry; the $^1A_{1g}$ state is the transition state for the cyclooctatetraene ring inversion.[36] The photoelectron spectrum is rich in vibrational structure revealing several vibrational modes associated with COT in the transition state.

The theoretical treatment for nonadiabatic electron transfer used in the present analysis is the Levich modification to Marcus theory.[37] Additionally, excited vibrational states of the electron acceptor are included using the approaches outlined by Jortner and Van Duyne, yielding the following equation for the electron-transfer rate constant:[38,39]

$$k_{et} = \sqrt{\frac{\pi}{\hbar^2 \lambda_s k_B T}} * |V|^2 * \sum_{w=0}^{\infty} (e^{-S} S^w / w!) \exp - \left[\frac{(\Delta G^\circ + \lambda_s + w\hbar\omega)^2}{4\lambda_s k_B T}\right] \quad (6)$$

Here, V is the electronic coupling matrix element. The ω value is the high-frequency vibrational mode associated with skeletal reorganizations of the product after the transfer. The summation over w accounts for the participation of excited ω modes in the product state. S is given by

$$S = \frac{\lambda_v}{\hbar\omega} \quad (7)$$

and describes the electron-vibration coupling strength.

In order to determine the transfer-promoting mode, ω, a simple estimate of λ_v is made for both the acetate radical and the benzhydrylium radical at the B3LYP/6-31G* level of calculation; the mode responsible for the largest reorganization energy is assigned to λ. To calculate λ_v, the energies of the two radicals and the two ions are first minimized. Then, the single-point energies of the anion and cation at their respective optimal radical geometries are calculated. The difference between the minimized ion energy and the ion energy at the radical geometry is assigned to λ_v. This estimate results in a λ_v of 1.5 kcal/mol for the benzhydrylium radical and 15.9 kcal/mol for the acetate radical. Since λ_v is larger for the acetate, most of the reorganization associated with electron transfer occurs in the acetate and therefore ⎤ is assigned to the vibrational frequency involved in acetate rearrangement from the radical to the anion. The largest change in geometry following electron transfer is the C−C bond length, which lengthens from 1.496 to 1.576 Å. The vibration most intimately involved in the acetate rearrangement will be the C−C stretch; an AM1 level calculation of acetate anion vibrations yields a frequency of $\omega = 962$ cm^{-1} for this stretch.

(36) Wenthold, P. G.; Hrovat, D. A.; Borden, W. T.; Lineberger, W. C. *Science* **1996**, *272*, 1456−1459.
(37) Levich, V. G. *Adv. Electrochem. Electrochem. Eng.* **1966**, *4*, 249−280.
(38) Kestner, N. R.; Logan, J.; Jortner, J. *J. Phys. Chem.* **1974**, *78*, 2148−2166.
(39) Fischer, S. F.; Duyne, R. P. v. *Chem. Phys.* **1977**, *26*, 9−16.

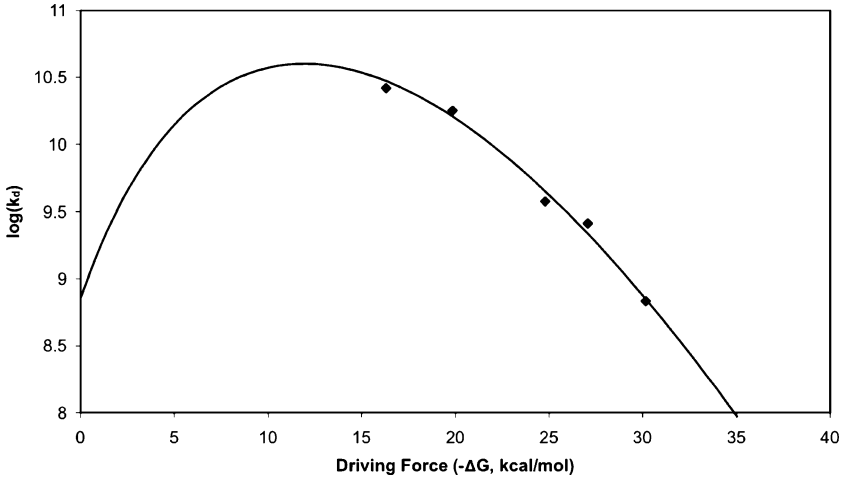

Figure 2. Fit of the nonadiabatic electron-transfer model, eq 6, to k_d as a function of driving force, $-\Delta G$, in the solvent propionitrile. Fitting parameters given in Table 4.

Table 4. Fitting Parameters Derived from the Model for Nonadiabatic Electron Transfer: Solvent Reorganization Energy (λ_s), Vibrational Reorganization Energy (λ_v), and Electronic Coupling (V)

	acetonitrile	propionitrile	butyronitrile
λ_s (kcal/mol)	5	4.3	4.3
λ_v (kcal/mol)	8.8	8.8	8.8
V (kcal/mol)	0.036	0.036	0.036

To complete the fit to theory, V, λ_s, and λ_v are varied in the correlation of the rate constant for electron transfer with driving force, ΔG. In general, V controls the value of the maximum rate constant, λ_s and λ_v control the location of the maximum rate constant along the driving force axis, and λ_v controls the breadth of the curve (larger λ_v values lead to "softer" curves). The fitting parameters for benzhydryl acetates are given in Table 4, and Figure 2 is an example fit.

The formalism for nonadiabatic electron transfer accurately describes the correlation of the rate constant for electron transfer with driving force. Also, the measured rate constants are clearly in an inverted region, where the transfer rate decreases as reaction driving force increases. Since the rate constants do not span the entire turnover from normal to inverted region, the fitting parameters should be interpreted with caution. As expected, the λ_s fit values decrease with decreasing solvent polarity.[40] Additionally, a comparison to the parameters obtained by a similar fit done by Pincock and co-workers on the rate of conversion of benzyl acetate radical pairs to ion pairs in methanol is useful.[21] The Pincock study calculates values of 4.6 kcal/mol for λ_s, 2.4 kcal/mol for λ_v, and 0.0074 kcal/mol for V. The λ_s values calculated in this study are very similar to the values calculated by Pincock. The Pincock λ_s value is twice λ_v, whereas, in the present study, the λ_v value is a little less than twice the λ_s value. This discrepancy is puzzling considering both studies involve the acetate radical reorganizing, and our analysis indicates that this reorganization is dominant. Last, the V value calculated in the present study is five times larger than the value in the Pincock study. While the maximum rate of electron transfer obtained by Pincock was 3.3×10^9 s^{-1}, the maximum observed in this study is more than an order of magnitude larger at 3.96×10^{10} s^{-1} which is reflected in the larger value of V obtained from the present analysis.

(40) Gould, I. R.; Noukakis, D.; Gomez-Jahn, L.; Young, R. H.; Goodman, J. L.; Farid, S. *Chem. Phys.* **1993**, *176*, 439.

Conclusions

The aim of the present study was to address three questions raised from the consideration of the valence bond reaction diagram associated with the S_N1 reaction mechanism. It is established that, within the benzhydryl acetate geminate radical pair, as electron withdrawing substituents are replaced by electron donating substituents, the electronic interaction within the geminate radical pair increases. In addition with this change in substituents, the energy splitting between the transition state for bond heterolysis and geminate radical pair also increases, a finding in accord with Kim−Hynes valence bond calculations. Finally the mechanism for the decay of the geminate radical pair onto the ground state surface can be ascribed to a nonadiabatic electron-transfer process; for the present molecular system, the kinetics for the process occurs within the inverted regime for electron transfer.

Acknowledgment. This work is supported by a grant from the National Science Foundation, No. CHE-0408265. L.R.H. acknowledges support from the University of Colorado OSEP, an NSF-IGERT program.

Supporting Information Available: Contains the warning for solvents, the synthesis and characterization of the compounds studied, and the calculated energies and coordinates for the various benzhydryl derivatives. The material is available free of charge via the Internet at http://pubs.acs.org.

JA077105N